

RESEARCH

Open Access



Role of NAT10-mediated ac⁴C acetylation of ENO1 mRNA in glycolysis and apoptosis in non-small cell lung cancer cells

Yanqing Yuan¹, Na Li¹, Jingui Zhu¹, Chun Shao¹, Xiangbo Zeng¹ and Daijiao Yi^{1*}

Abstract

Background Abnormal expression of N-acetyltransferase 10 (NAT10) has been shown to promote the progression of various tumors, including non-small cell lung cancer (NSCLC). This study was designed to investigate the role of NAT10 in NSCLC and the underlying mechanism.

Methods Reverse transcription-quantitative polymerase chain reaction and Western blot were used to analyze the levels of NAT10 in NSCLC cell lines. The cell viability, proliferation, and apoptosis of A549 and PC9 cell lines were detected by cell counting kit-8, colony formation, and flow cytometry. N4-acetylcytidine (ac⁴C)-RNA immunoprecipitation assay was performed to detect the level of ac⁴C of α -enolase (ENO1) mRNA in A549 and PC9 cell lines. The relationship between NAT10 and ENO1 was performed by dual-luciferase reporter assay.

Results NAT10 was increased in NSCLC cell lines. The ac⁴C level of ENO1 mRNA in A549 and PC9 cell lines was downregulated after NAT10 inhibition. Knockdown of NAT10 inhibited cell viability and glycolysis and promoted cell apoptosis in A549 and PC9 cell lines, and the results were reversed after ENO1 overexpressing.

Conclusions NAT10 regulated glycolysis and apoptosis in NSCLC via ac⁴C acetylating ENO1, which might provide new ideas for the clinical treatment of NSCLC.

Keywords Non-small cell lung cancer, NAT10, ENO1, ac⁴C, Glycolysis, Apoptosis

Background

Lung cancer is the most common cause of cancer-related deaths worldwide. More than 85% of lung cancer cases are classified as non-small cell lung cancer (NSCLC), with a predicted 5-year survival rate of only about 15.9% [1]. Over the past two decades, multidisciplinary efforts and technological advances have enhanced our understanding of the molecular mechanisms of NSCLC [2].

In addition, molecularly targeted therapies and immunotherapy have improved the prognosis of NSCLC [3]. However, targeted therapies are only effective in fewer than 25% of patients, and drug resistance is almost universal during treatment [4]. Besides, other treatments, such as adjuvant chemotherapy, showed modest survival benefits at different stages, but more than half of patients will relapse [5]. Thus, novel treatments for NSCLC are worth further investigation and exploration.

Various RNA modifications at the post-transcriptional stage play key roles in regulating RNA stability, localization, transport, and translation [6–8]. N4-acetylcytidine (ac⁴C) is a newly conserved acetylation modification discovered in both eukaryotes and prokaryotes. Early

*Correspondence:

Daijiao Yi
yidaijiao725@126.com

¹The Second People's Hospital of Hunan Province (Brain Hospital of Hunan Province), No. 427, Section 3, Furong Middle Road, Changsha 410000, Hunan Province, China



© The Author(s) 2024. **Open Access** This article is licensed under a Creative Commons Attribution-NonCommercial-NoDerivatives 4.0 International License, which permits any non-commercial use, sharing, distribution and reproduction in any medium or format, as long as you give appropriate credit to the original author(s) and the source, provide a link to the Creative Commons licence, and indicate if you modified the licensed material. You do not have permission under this licence to share adapted material derived from this article or parts of it. The images or other third party material in this article are included in the article's Creative Commons licence, unless indicated otherwise in a credit line to the material. If material is not included in the article's Creative Commons licence and your intended use is not permitted by statutory regulation or exceeds the permitted use, you will need to obtain permission directly from the copyright holder. To view a copy of this licence, visit <http://creativecommons.org/licenses/by-nc-nd/4.0/>.

studies suggest that ac⁴C modification mainly exists on tRNAs and 18 S rRNAs; later, it has been found that there is also a large amount of ac⁴C on mRNAs [9, 10]. Ac⁴C shows antiviral and anti-inflammatory effects on many diseases [11, 12]. Importantly, ac⁴C is a potential biomarker for cancers, which is associated with the occurrence, progression, and prognosis of many cancers [13]. N-acetyltransferase 10 (NAT10), a nucleolar acetyltransferase, is the only known enzyme that catalyzes the ac⁴C modification on its target RNAs [14]. Ac⁴C can promote mRNA stability, substrate translation, and cell proliferation under the catalysis of NAT10 and its auxiliary enzymes [15]. A previous study indicates that NAT10 is a possible prognostic marker and a potential target for the treatment of NSCLC [16]. Additionally, a previous study indicates that NAT10-mediated upregulation of growth arrest-specific 5 (GAS5) facilitates immune cell infiltration in NSCLC [17]. Besides, NAT10-mediated ac⁴C mRNA modification promotes the progression of various cancers [18, 19]. NAT10 promotes cancer metastasis by increasing related-mRNA stability in an ac⁴C-dependent manner [20].

Altered energy metabolism is a biochemical fingerprint of cancer cells that represents one of the “hallmarks of cancer” [21]. Glycolysis is a common pathway in living cells. In cancer cells, glycolysis is always enhanced to meet the growing energy needs [22]. Tumor glycolysis is a major promoter of cancer occurrence and progression, and high tumor glycolysis activity is associated with low overall survival [23]. The genes associated with glycolysis are highly expressed in cancer tissues [24]. α -Enolase (ENO1) is a glycolytic enzyme that exists on the cell surface and cytoplasm, which can maintain tumor cell proliferation and inhibit apoptosis [25]. ENO1 promotes glycolysis and enhances lung tumor progression through RNA modifications or related signaling pathways [26, 27]. Whereas, the role of ac⁴C modification of ENO1 in NSCLC is largely unknown.

This study aimed to investigate the role of NAT10 in NSCLC, and further investigate the mechanism of downstream gene ENO1 in glycolysis and apoptosis, which might provide a potential therapeutic intervention strategy for NSCLC.

Methods

Bioinformatics analysis

The expression of NAT10 in normal and lung squamous cell carcinoma (LUSC) or lung adenocarcinoma (LUAD) tissues was analyzed using the The University of Alabama at Birmingham CANcer data analysis Portal (UALCAN) database (<https://ualcan.path.uab.edu/analysis.html>). The LinkedOmics database (<https://www.linkedomics.org/login.php>) showed genes positively and negatively related to NAT10.

Cell culture

The routine culture of the cells was carried out in reference to a previous study [28]. NSCLC cell lines (H157, PC9, H460, and A549) and human bronchial epithelial cells (BEAS-2B) were purchased from the Cell Bank of the Chinese Academy of Sciences (Shanghai, China) and cultured in Dulbecco's modified Eagle's medium (DMEM, Gibco, NY, USA) containing 10% heat-inactivated fetal bovine serum (FBS, Gibco), 100 U/mL penicillin and 100 μ g/mL streptomycin (Sigma) and incubated in a humidified incubator at 37 °C with 5% CO₂.

Cell transfection

NAT10 short hairpin (sh) RNA (sh-NAT10), negative control shRNA (sh-NC), negative control overexpression (oe-NC), and ENO1 overexpression (oe-ENO1) plasmids were synthesized (GenesScript Biotechnology Co. Ltd., Nanjing, China). The cells (5×10^5 cells/well) were inoculated in a six-well plate (Beyotime). After the cell confluence reached 80%, transfection was performed using Lipofectamine 2000 (Sigma) according to the manufacturer's instructions. Specifically, the plasmids or shRNAs were diluted in Opti-MEM reduced serum medium (Gibco), and Lipofectamine 2000 was diluted in a separate tube of Opti-MEM. The diluted plasmids or shRNAs were then mixed with the diluted Lipofectamine 2000 and incubated at room temperature for 20 min to allow complex formation. The transfection mixture was added dropwise to the cells, and the plates were gently swirled to ensure even distribution. The cells were incubated at 37 °C with 5% CO₂ for 48 h. After the transfection period, the efficiency of transfection was assessed by reverse transcription-quantitative polymerase chain reaction (RT-qPCR) using specific primers for NAT10 and ENO1.

RT-qPCR

Total RNA from cells was extracted by TRIzol reagent (Yeason). Then, RNA was reverse transcribed into cDNA using the Hifair[®] AdvanceFast 1st Strand cDNA Synthesis Kit (Yeason), and the qPCR amplification experiment was performed using the Hieff[®] qPCR SYBR Green Master Mix (Yeason) with the reaction conditions: 95 °C for 5 min, 40 cycles of 95 °C for 10 s, 60 °C for 30 s, and a cycle of 72 °C for 20 s. The gene expression was calculated by the $2^{-\Delta\Delta CT}$ method. Primers used in this study are listed as follows: N-acetyltransferase 10 (NAT10), forward, 5'-ATAGCAGCCACAAACATTTCGC-3' and reverse, 5'-ACACACATGCCGAAGGTATTG-3'; α -enolase (ENO1), forward, 5'-CCTGCCCTGGTTAGCAAGAA-3' and reverse, 5'-GGCGTTCGCACCAAACTTAG-3'; glyceraldehyde-3-phosphate dehydrogenase (GAPDH), 5'-TGTGGGCATCAATGGATTTGG-3' and reverse, 5'-ACACCATGTATTCCGGGTCAAT-3'.

Western blot

Protein extraction was performed by lysing the cells in RIPA buffer (Thermo Fisher Scientific, Waltham, MA, USA). The lysates were centrifuged at 12,000 rpm for 10 min at 4 °C, and the supernatants were collected. Protein concentrations were measured using the BCA Protein Assay kit (Thermo Fisher). Equal amounts of protein (30 µg) were loaded onto 10% SDS-PAGE gels and separated by electrophoresis. The proteins were then transferred to PVDF membranes using a semi-dry transfer apparatus. Membranes were blocked with 5% non-fat milk in Tris-buffered saline with Tween-20 for 1 h at room temperature. Primary antibodies against NAT10 (ab194297; 1/2000; Abcam Cambridge, MA, USA), ENO1 (ab227978; 1/1000; Abcam), and β-actin (ab8227; 1/5000; Abcam) were diluted according to the manufacturer's instructions and incubated with the membranes overnight at 4 °C. After washing three times with TBST, the membranes were incubated with HRP-conjugated secondary antibody (ab6721; 1/10,000; Abcam) for 1 h at room temperature. Following additional washes, the proteins were visualized using enhanced chemiluminescence (ECL) substrate (Thermo Fisher) and detected with a ChemiDoc imaging system (Bio-Rad, Hercules, CA, USA). GAPDH was used as a loading control to normalize the protein expression levels. Band intensities were quantified using Image J software.

Cell counting kit-8 (CCK-8) assay

Cell viability was detected using the CCK-8 kit (Beyotime) according to the manufacturer's instructions. Briefly, cells were seeded in 96-well plates at a density of 5×10^3 cells per well and allowed to adhere overnight. Afterwards, 10 µL of CCK-8 solution was added to each well, and the plates were incubated at 37 °C for 2 h. The absorbance was then measured at 450 nm using a microplate reader (Thermo Fisher). The results were expressed as the percentage of viable cells compared to the control group.

Colony formation assay

To assess the proliferation capacity of A549 and PC9 cells, the colony formation assay was conducted. A549 and PC9 cells were trypsinized and counted using a hemocytometer. Cells were then seeded in 6-well plates at a low density (approximately 500 cells per well) to ensure the formation of distinct colonies. After 14 days of incubation at 37 °C in a humidified atmosphere containing 5% CO₂, the medium was removed, and the cells were gently washed with PBS. The colonies were fixed with 70% ethanol (Beyotime) for 10 min and stained with 0.5% crystal violet solution (Beyotime) dissolved in 20% methanol for 30 min at room temperature. Images of

representative wells were captured using a digital camera, and the number of colonies was quantified.

Detection of apoptosis rate

The apoptosis rate of A549 and PC9 cell lines was assessed by fluorescein isothiocyanate (FITC) and propidium iodide (PI) double staining solution using a commercial Apoptosis Detection Kit (Yeason) according to the instructions. Cells were harvested and washed twice with cold phosphate-buffered saline (PBS), then resuspended in $1 \times$ binding buffer at a concentration of 1×10^6 cells/mL. A total of 100 µL of the cell suspension was transferred to a new tube, and 5 µL of annexin V-FITC and 5 µL of PI were added. The samples were gently mixed and incubated in the dark for 15 min at room temperature. After incubation, 400 µL of $1 \times$ binding buffer was added to each tube to adjust the volume. The cell samples were then analyzed using a FACS CantoII flow cytometer (BD Biosciences, CA, USA). The excitation wavelength for flow cytometry was set at 488 nm. The cell apoptosis rate was quantified using BD FACSDiva software. To ensure reliability, flow cytometry was conducted three times, with three biological repetitions for each experiment.

¹⁸F-fluorodeoxyglucose (FDG) uptake

The transfected 1×10^5 A549 and PC9 cell lines were cultured in six-well cell culture plates until the cells reached approximately 80-90% confluency. Then, the cells were incubated in 2 mL DMEM containing ¹⁸F-FDG (148 kBq [4 µCi/mL]) for 1 h at 37 °C and 5% CO₂. After incubation, the media was removed, and the cells were washed twice with ice-cold PBS to remove any unincorporated ¹⁸F-FDG. Cell lysates were prepared by adding 1 mL of trypsin to each well and incubating the cells at 37 °C for 5 min. The trypsinized cells were collected and centrifuged at 1,000 rpm for 5 min at 4 °C to pellet the cells. The supernatant was discarded, and the cell pellets were resuspended in 1 mL of RIPA buffer containing protease inhibitors. The radioactivity of the whole-cell lysates was determined using a gamma counter (ZonKia Scientific Instruments Co. LTD., Hefei, China). The protein content of the lysates was measured using the BCA assay, and the results were normalized to the corresponding protein amounts. All experiments were performed in triplicate to ensure reproducibility.

Lactate production measurement

For the measurement of lactate levels, transfected A549 and PC9 cell lines were seeded at a density of 1×10^5 cells per well in six-well plates. The cells were allowed to adhere and grow for 24 h. After this period, the cell culture medium was carefully collected and centrifuged at 1,000 rpm for 5 min at 4 °C to remove any cellular debris.

The supernatant was then used for lactate quantification using the lactate assay kit (Jiancheng Bioengineering Institute, Nanjing, China) according to the manufacturer's instructions. Briefly, the assay reagents were prepared by mixing the lactate oxidase, peroxidase, and color developer solutions as specified in the kit. Standard solutions of lactate were also prepared to generate a standard curve. Aliquots of the cell culture supernatant and standard solutions were added to a 96-well plate, and the assay reagents were added to each well. The plate was incubated at room temperature for 30 min to allow the color development. The absorbance was then measured at 530 nm using the Synergy HTX Multi-Mode Microplate Reader (Agilent Technology Co. LTD., Beijing, China). To normalize the lactate levels to protein content, the cells remaining in the six-well plates were lysed using RIPA buffer containing protease inhibitors. The protein concentration was determined using the BCA assay according to the manufacturer's instructions. The lactate levels were then normalized to the corresponding protein amounts. All experiments were performed in triplicate to ensure reproducibility.

Measurement of extracellular acidification rate (ECAR) and oxygen consumption rate (OCR)

According to previous studies [29, 30], the ECAR and OCR of A549 and PC9 cell lines were assessed using the Seahorse XFe24 Flux Analyzer (Seahorse Bioscience, Agilent) to evaluate glycolytic fluxes. The glycolytic stress test kit (Seahorse) and mitochondrial stress test kit (Seahorse) were used for ECAR and OCR detection, respectively. Briefly, the cells were plated at a density of 1×10^5 cells/well in the Seahorse XF cell culture microplate and allowed to adhere overnight. The next day, the media was changed to Seahorse XF Base Medium, pH-adjusted to 7.4, and the cells were incubated at 37 °C without CO₂ for 1 h to equilibrate.

For the mitochondrial stress test, sequential compound injections were made at the following final concentrations: oligomycin (1 μM), carbonyl-cyanide p-trifluoromethoxyphenylhydrazone (FCCP) (0.3 μM), and rotenone/antimycin A (Rote/AA) (0.1 μM). For the glycolytic stress test, sequential compound injections were made at the following final concentrations: glucose (10 mM), oligomycin (0.5 μM), and 2-Deoxy-D-glucose (2-DG) (50 mM). Each injection was also followed by a 3-minute mixing period and a 3-minute measurement period. Post assay, wells were washed, cells lysed, and the BCA assay was performed for protein content. These readouts were normalized to corresponding protein amounts.

Ac⁴C RNA immunoprecipitation (RIP)

The ac⁴C RIP assay was performed according to a previous study [31] using a GenSeq ac⁴C RIP kit (Cloudseq Biotech, Shanghai, China) following the manufacturer's instructions. Protein A/G magnetic beads (Thermo Fisher) were activated with purification buffer and conjugated with 5 μg of anti-ac⁴C antibody (Abcam), and 5 μg of rabbit IgG antibody (Abcam) at room temperature for 2 h. After that, the beads were washed with purification buffer three times. In addition, 10% of the cell lysate was saved as input at -80 °C. Antibody-conjugated A/G magnetic beads were incubated with 45% of cell lysate, 0.25 M EDTA, and RNase inhibitor (Sigma) at 4°C for 4 h separately. Then, the beads were washed with purification buffer another three times, and all the solution was discarded. Later, the A/G magnetic beads were incubated with lysis buffer, 10% SDS, and 10 mg/ml proteinase K at 55 °C for 30 min to purify mRNA. Moreover, reverse transcription was performed, and qPCR was followed to test the binding of target RNA.

Dual-luciferase reporter assay

The cDNA containing full-length 3'-untranslated regions (UTR) of ENO1 was cloned into the pGL3 luciferase reporter vector (Promega, USA), to obtain pGL3-ENO1-wild type (WT). pGL3-ENO1-mutant type (MUT) plasmid was obtained by the introduction of mutations into pGL3-ENO1-WT using the QuikChange II Site-Directed Mutagenesis kit (Agilent). Next, the sh-NAT10 or a sh-NC were co-transfected with either pGL3-ENO1-WT or pGL3-ENO1-MUT into A549 and PC9 cell lines using Lipofectamine 2000 according to the manufacturer's instructions. Cells were seeded in 24-well plates at a density of 5×10^4 cells per well and allowed to adhere overnight. For transfection, 1 μg of each plasmid and 50 nM of shRNA were mixed with 2.5 μL of Lipofectamine 2000 in Opti-MEM reduced serum medium and incubated for 20 min at room temperature. The transfection mixture was then added to the cells, and the cells were incubated at 37 °C with 5% CO₂ for 48 h. Afterwards, the cells were lysed using the Passive Lysis Buffer provided in the Dual-Luciferase[®] Reporter Assay System (Promega). Then, luciferase activity was measured using Dual-Luciferase[®] Reporter Assay System (Promega) and normalized to the activity of Renilla luciferase. The ratio of firefly/Renilla luciferase activity was used as the relative luciferase activity.

RNA stability assessment

RNA stability assessment was performed to verify the stability of ENO1 after NAT10 silencing in A549 and PC9 cell lines. A549 and PC9 cell lines were treated with actinomycin (Act) D (0.5 μg/ml, Sigma), an inhibitor for RNA transcription, then existing ENO1 expression was

detected at different time points (0, 8, 16, and 24 h) using qPCR.

Statistical analysis

The SPSS 21.0 software was used to analyze data. Data are expressed as mean \pm standard deviation (SD). Student's t-test was used for comparison between the two groups. One-way analysis of variance (ANOVA) was used for comparison among groups. Statistical analyses were performed using GraphPad Prism software (v8.0.1,

GraphPad Software Inc., San Diego, CA, USA). $p < 0.05$ indicates that the difference is statistically significant.

Results

High expression of NAT10 in NSCLC

Bioinformatic analysis using the UALCAN database showed that the expression of NAT10 was upregulated in LUAD (Fig. 1A) and LUSC (Fig. 1B) tissues compared with that in normal tissues. NAT10 mRNA and protein levels were increased in NSCLC cell lines (PC9, A549,

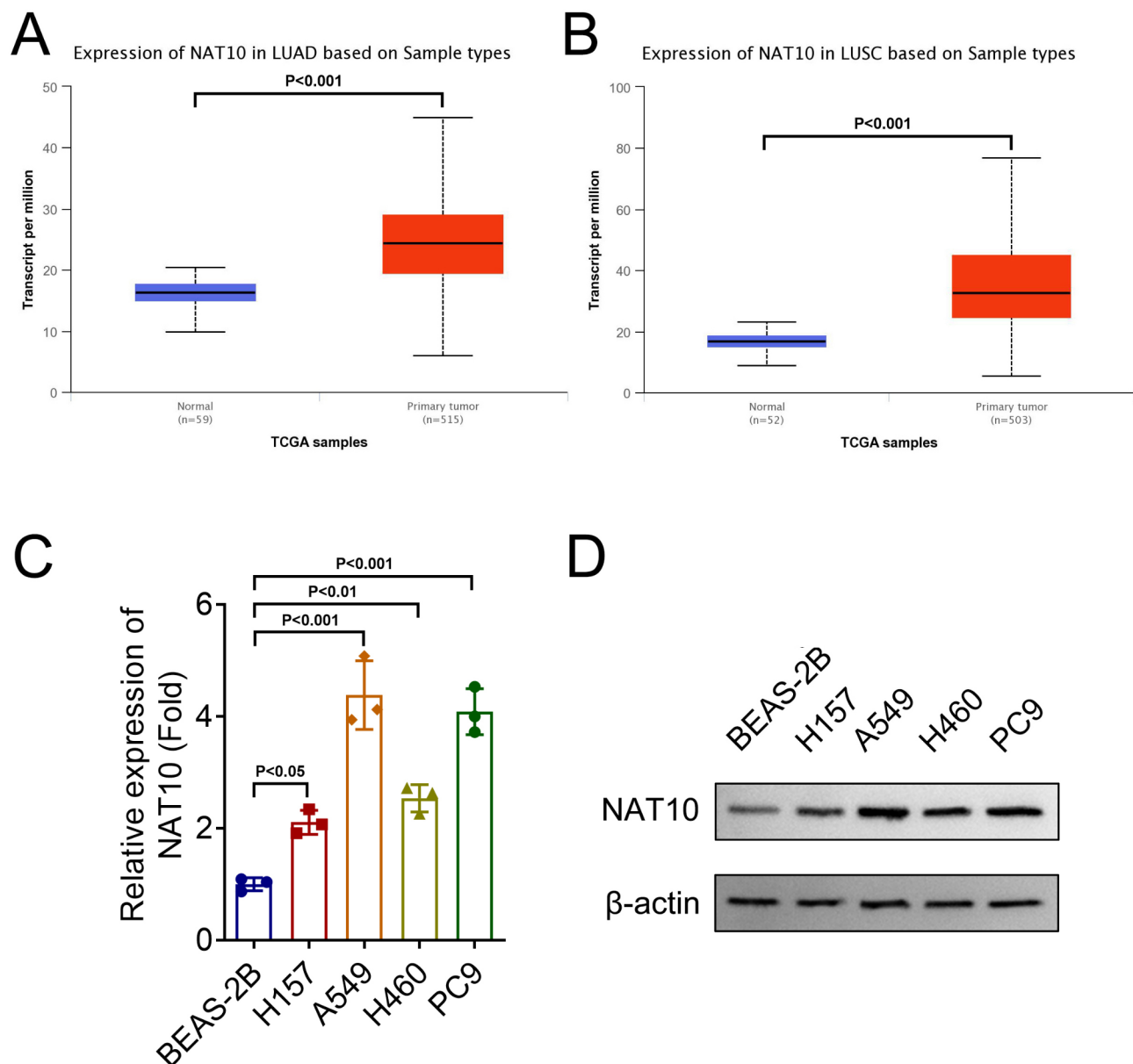


Fig. 1 High expression of NAT10 in NSCLC. **A**, The UALCAN database was used to analyze the NAT10 expression in LUAD ($n = 515$) and normal tissues ($n = 59$); **B**, The UALCAN database was used to analyze the NAT10 expression in LUSC ($n = 503$) and normal tissues ($n = 52$); **C**, RT-qPCR and **D**, Western blot were used to analyze the expression levels of NAT10 in NSCLC cell lines (H157, H460, A549, and PC9) and BEAS-2B cells ($n = 3$). **NAT10**, N-acetyltransferase 10; **LUAD**, lung adenocarcinoma; **LUSC**, lung squamous cell carcinoma; **NSCLC**, non-small cell lung cancer; **UALCAN**, The University of Alabama at Birmingham CANcer data analysis Portal; **RT-qPCR**, reverse transcription-quantitative polymerase chain reaction

H460, and H157) compared with that in BEAS-2B cells (Fig. 1C and D). PC9 and A549 cell lines were chosen for followed experiments.

Knockdown of NAT10 inhibited cell viability and glycolysis and promoted cell apoptosis of A549 and PC9 cell lines

To further verify the effect of NAT10 on NSCLC cellular processes, we transfected sh-NAT10 into A549 and PC9

cell lines, and its mRNA and protein levels were down-regulated (Fig. 2A and B). The cell viability of A549 and PC9 cell lines was suppressed after NAT10 inhibition (Fig. 2C). Colony formation assay results showed that NAT10 knockout decreased the colony number of A549 and PC9 cell lines (Fig. 2D and E). Besides, flow cytometry results showed that NAT10 knockdown increased the apoptosis rate of A549 and PC9 cell lines (Fig. 2F

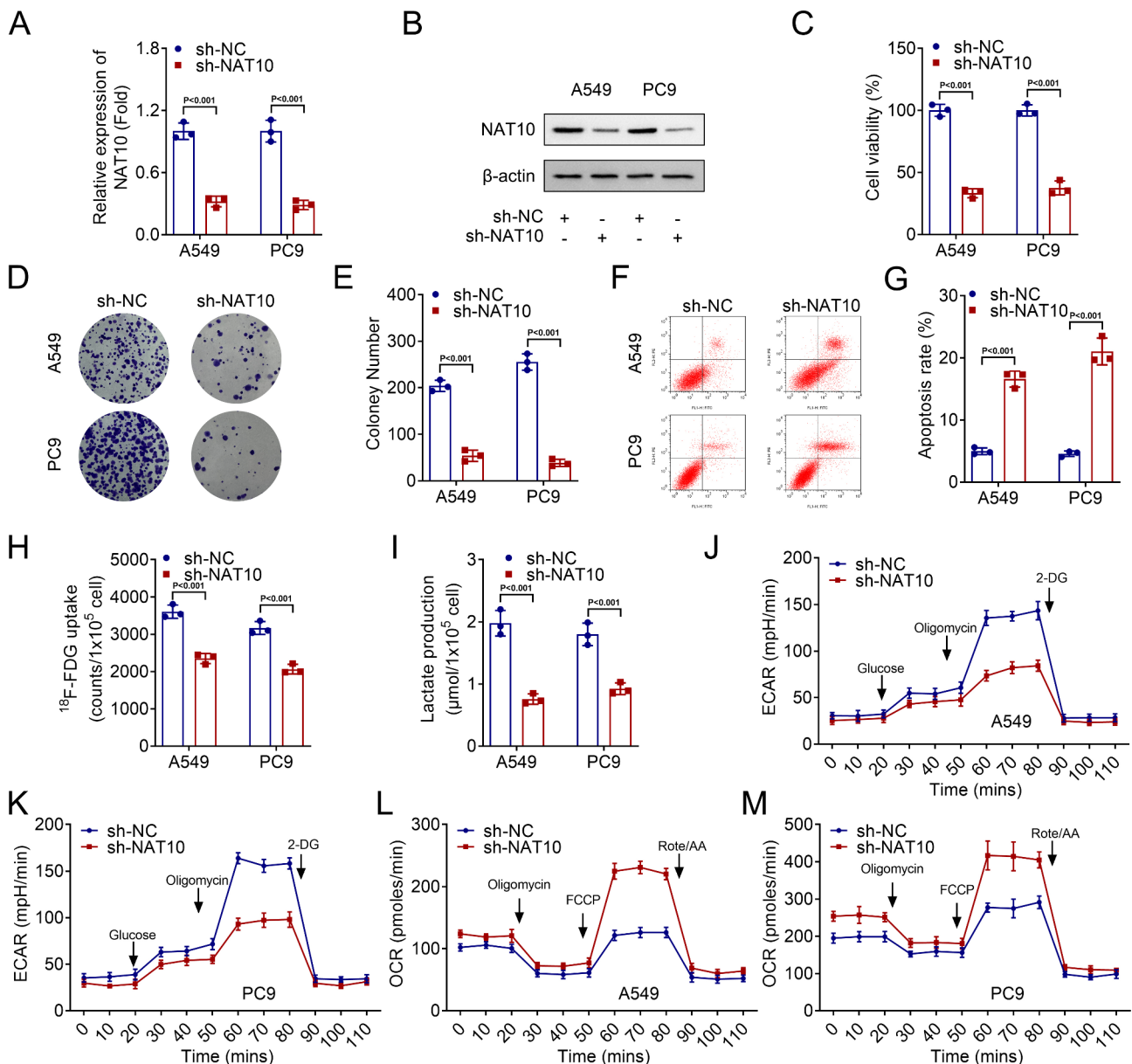


Fig. 2 Knockdown of NAT10 inhibited cell viability and glycolysis and promoted cell apoptosis of A549 and PC9 cell lines. The transfection efficiency of sh-NAT10 in A549 and PC9 cell lines was detected by **A**, RT-qPCR and **B**, Western blot; **C**, CCK-8 assay was performed to assess the cell viability of A549 and PC9 cell lines; **D**, Colony formation assay was conducted to analyze the cell proliferation in A549 and PC9 cell lines; **E**, Quantification of colony number of A549 and PC9 cell lines in each group; **F**, Flow cytometry was performed to detect the apoptosis of A549 and PC9 cell lines; **G**, The apoptosis rate of A549 and PC9 cell lines; **H**, The ^{18}F -FDG uptake in A549 and PC9 cell lines; **I**, The lactate production of A549 and PC9 cell lines was detected by specific kit; The ECAR in **J**, A549 and **K**, PC9 cell lines. The OCR in **L**, A549 and **M**, PC9 cell lines. ($n = 3$). **NAT10**, N-acetyltransferase 10; **RT-qPCR**, reverse transcription-polymerase chain reaction; **CCK-8**, cell counting kit-8; **ECAR**, extracellular acidification rate; **OCR**, oxygen consumption rate; ^{18}F -**FDG**, ^{18}F -fluorodeoxyglucose; **sh-RNA**, short hairpin RNA

and G). In addition, silencing NAT10 decreased the ^{18}F -FDG uptake (Fig. 2H), lactate production (Fig. 2I), ECAR (Fig. 2J and K) and OCR (Fig. 2L and M) in A549 and PC9 cell lines.

ENO1 was a downstream regulatory target of NAT10-mediated ac^4C acetylation in A549 and PC9 cell lines

The LinkedOmics database was used to analysis the genes positively and negatively related to NAT10 (Fig. 3A). ENO1 is a gene positively related to NAT10, which has not been researched in NSCLC before. In addition, ENO1

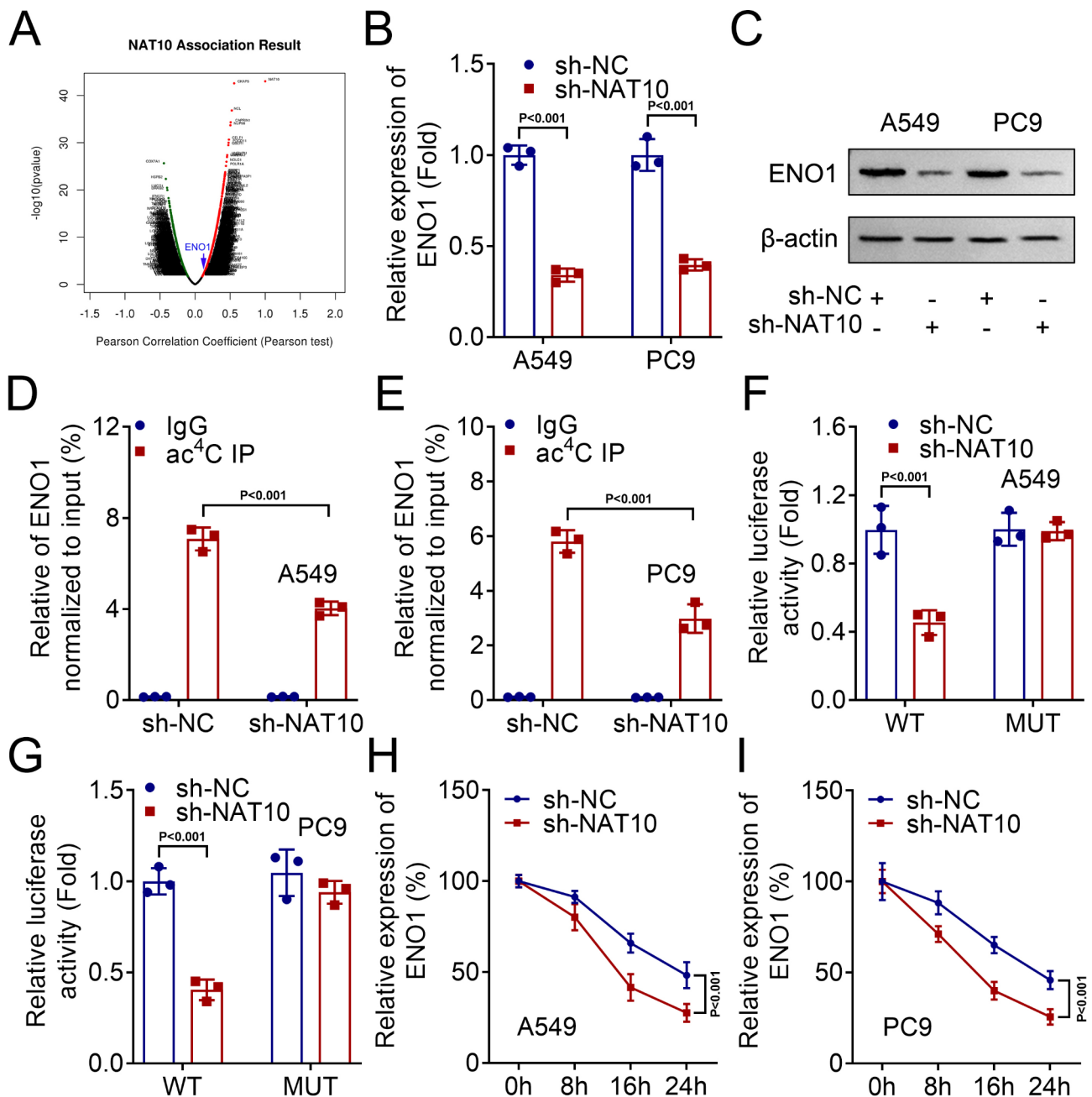


Fig. 3 ENO1 was a downstream regulatory target of NAT10-mediated ac^4C acetylation in A549 and PC9 cell lines. **A**, Genes positively and negatively related to NAT10 were obtained using the Linkedomics database; The mRNA and protein levels of ENO1 in A549 and PC9 cell lines were detected by **B**, RT-qPCR and **C**, Western blot after NAT10 knockdown; ac^4C -RIP assay was performed to detect ENO1 ac^4C expression in **D**, A549 and **E**, PC9 cell lines; Dual-luciferase reporter assay was used to evaluate the binding of NAT10 and ENO1 in **F**, A549 and **G**, PC9 cell lines; RNA stability assay was used to detect the existing NAT10 expression when actinomycin D treated at different time points (0, 8, 16, and 24 h) in **H**, A549 and **I**, PC9 cell lines. ($n=3$). **NAT10**, N-acetyltransferase 10; **RT-qPCR**, reverse transcription-polymerase chain reaction; **ENO1**, α -enolase; **NSCLC**, non-small cell lung cancer; **RIP**, RNA immunoprecipitation; **ac^4C** , N4-acetylcytidine

is a glycolysis-related enzyme. Thus, ENO1 was chosen as the downstream target of NAT10 in this study. The mRNA and protein levels of ENO1 were inhibited after NAT10 inhibition in A549 and PC9 cell lines (Fig. 3B and C). Besides, ac⁴C-RIP assay indicated that silencing of NAT10 showed a lower level of ac⁴C of ENO1 mRNA in A549 and PC9 cell lines (Fig. 3D and E), compared with that in the sh-NC group. Dual-luciferase reporter assay results indicated that the significant reduction in luciferase activity in the WT constructs compared to the MUT constructs supports that NAT10 interacted with ENO1 through the ac⁴C modification in A549 and PC9 cell lines (Fig. 3F and G). The observed differences in ENO1 mRNA stability between sh-NC and sh-NAT10 groups were statistically significant at all time points, indicating silencing NAT10 resulted in accelerated degradation of ENO1 mRNA in A549 and PC9 cell lines (Fig. 3H and I).

Overexpression of ENO1 reversed the decreases of cell viability and glycolysis and the increase of apoptosis in A549 and PC9 cell lines

Compared with the oe-NC group, ENO1 mRNA and protein levels were upregulated in the oe-ENO1 group (Fig. 4A and B). CCK-8 and colony formation assay results showed that relative to the oe-NC group, ENO1 overexpression increased the cell viability and proliferation (Fig. 4C-E). Additionally, compared with the oe-NC group, the apoptosis rate was upregulated in A549 and PC9 cell lines after ENO1 overexpressing (Fig. 4F and G). Moreover, compared with the oe-NC group, the ¹⁸F-FDG, lactate production, ECAR, and OCR in A549 and PC9 cell lines were upregulated when ENO1 was overexpressed (Fig. 4H-M).

Discussion

NAT10 is a therapeutic target for a variety of cancers [19, 32, 33]. In our study, NAT10 was upregulated in NSCLC cell lines. Similarly, Guo et al. [34] reveal high NAT10 expression in NSCLC tissues, cell lines and mouse xenograft models. In addition, Xu et al. [35] demonstrate that depletion of NAT10 inhibits the growth of xenograft tumors in nude mice. Moreover, an in vivo study implies that deficient NAT10 reduces tumor burden in xenografts and transgenic mouse models of bladder cancer [18]. Besides, high expression of NAT10 is associated with hepatitis, cirrhosis, and poor prognosis in patients with hepatocellular carcinoma [32]. These results suggested that NAT10 promoted the progression of various cancers including NSCLC.

To further explore the effect of NAT10 on biological behaviors of NSCLC cells, we successfully constructed NAT10 silenced A549 and PC9 cell lines. The results indicated that silencing of NAT10 inhibited cell viability and glycolysis and promoted apoptosis of A549 and

PC9 cell lines, suggesting that the knockdown of NAT10 inhibited the progression of NSCLC in vitro. Similarly, a recent study finds that NAT10 knockdown curtails proliferation, invasion, and migration, whereas NAT10 overexpression yields contrary effects in NSCLC [34]. Besides, another research has indicated that the proliferation ability, the healing of scratches, and invasion are suppressed, whereas apoptosis is promoted in tumor cells after NAT10 inhibition [18]. There are few studies on the effects of NAT10 on glycolysis. Interestingly, a recent study demonstrated that NAT10-mediated ac⁴C-modification enhances hypoxia tolerance of gastric cancer cells by promoting glycolysis addiction [36].

Then, we analyzed the genes related to NAT10. ENO1 is a gene positively related to NAT10, which has not been researched in NSCLC before; thus, we investigated the role of ENO1 in the present study. ENO1 is an oncogene [27, 37]. In this study, we found that silencing NAT10 inhibited the expression of ENO1 in A549 and PC9 cell lines, implying that ENO1 is a downstream regulatory target of NAT10 in NSCLC. Then, we found that the ac⁴C level of ENO1 mRNA was decreased after NAT10 knockdown in A549 and PC9 cell lines. ac⁴C mRNA modification catalyzed by NAT10 is associated with a variety of human diseases, especially cancers. Besides, the RNA stability of ENO1 was suppressed after NAT10 knockdown, suggesting that NAT10 could regulate the stability of ENO1 mRNA to improve the efficiency of mRNA transcription through NAT10-mediated ac⁴C-modified ENO1 mRNA acetylation. The findings are consistent with the reported studies indicating that NAT10-mediated ac⁴C mRNA plays regulatory roles in different diseases via acetylating target genes [32, 38].

In conclusion, our study demonstrated the role of NAT10-mediated ac⁴C modification of ENO1 mRNA acetylation in NSCLC, implying that NAT10 can be used as a biomarker to study the development and progression of NSCLC, or as a potential target for future treatment of NSCLC. The novelty of this study lies in the following points: While previous studies have explored the oncogenic functions of NAT10 in NSCLC, few research studies have linked its effects on glycolysis. Besides, we provide a detailed mechanistic understanding of how NAT10 mediates ac⁴C modification, which regulates the expression and activity of ENO1, a key glycolysis enzyme. This novel pathway offers new insights into the metabolic reprogramming driven by NAT10 in NSCLC. Thus, developing NAT10 or ac⁴C modification inhibitors could be promising therapeutic strategies for NSCLC clinical treatment. Moreover, combining NAT10 inhibitors with existing therapies, such as chemotherapy or immunotherapy, might enhance treatment efficacy.

However, there are some limitations to this study. For example, this study lacked clinical studies to explore

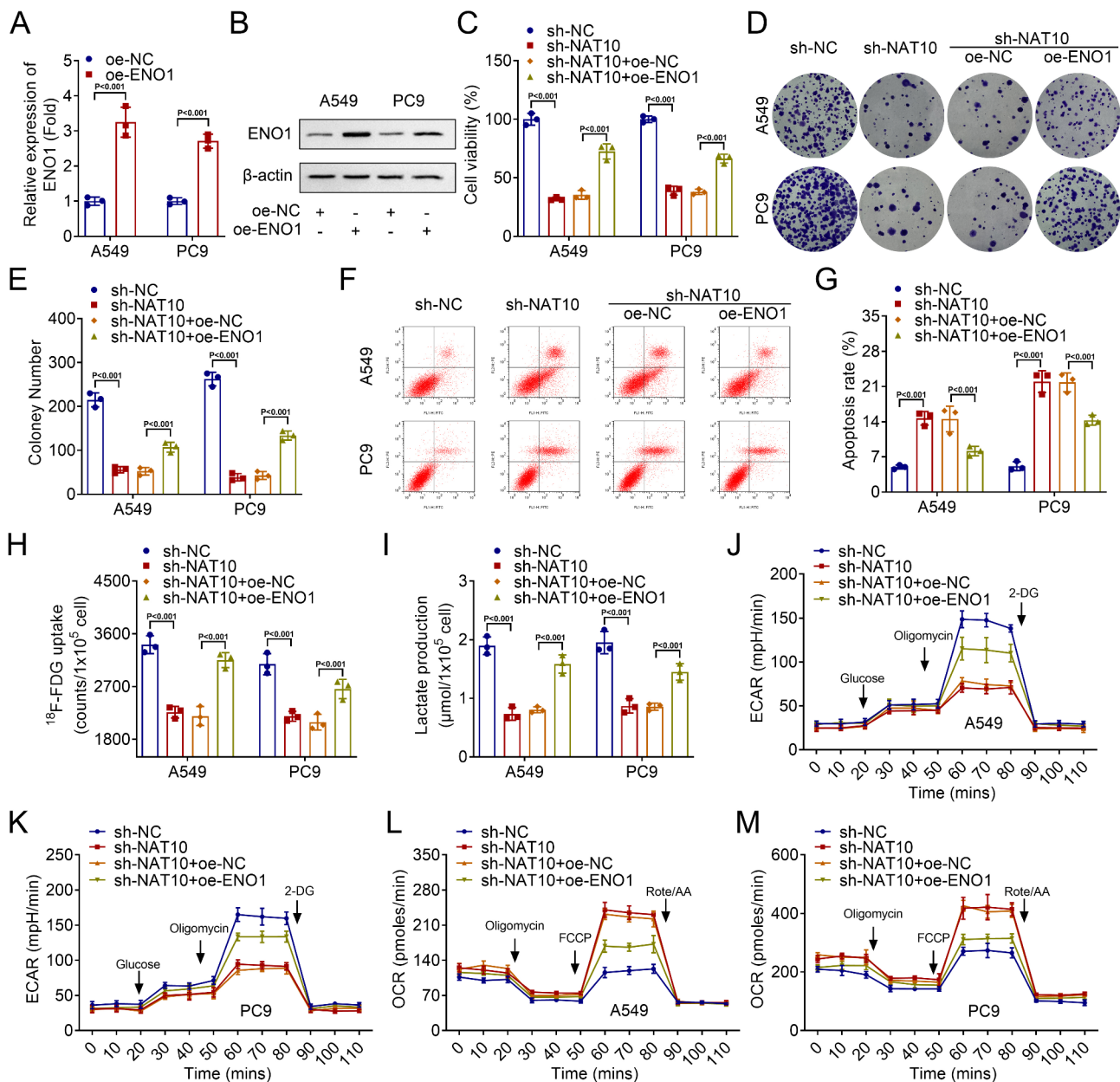


Fig. 4 Overexpression of ENO1 reversed the decreases of cell viability and glycolysis and the increase of apoptosis in A549 and PC9 cell lines. The transfection efficiency of ENO1 overexpression plasmids in A549 and PC9 cell lines was detected by **A**, RT-qPCR and **B**, Western blot; **C**, CCK-8 assay was performed to assess the viability of A549 and PC9 cell lines in each group; **D**, Colony formation assay was conducted to analyze the cell proliferation of A549 and PC9 cell lines in each group; **E**, Quantification of colony number of A549 and PC9 cell lines in each group; **F**, Flow cytometry was performed to detect the apoptosis of A549 and PC9 cell lines in each group; **G**, The apoptosis rate of A549 and PC9 cell lines in each group; **H**, The ^{18}F -FDG uptake of A549 and PC9 cell lines in each group; **I**, The lactate production of A549 and PC9 cell lines in each group was detected by specific kit; The ECAR in **J**, A549 and **K**, PC9 cell lines in each group; The OCR in **L**, A549 and **M**, PC9 cell lines in each group. ($n=3$). **NAT10**, N-acetyltransferase 10; **RT-qPCR**, reverse transcription-polymerase chain reaction; **CCK-8**, Cell counting kit-8; **ECAR**, extracellular acidification rate; **OCR**, oxygen consumption rate; ^{18}F -FDG, ^{18}F -fluorodeoxyglucose; **sh-RNA**, short hairpin RNA

whether expression of NAT10 was associated with survival in patients with NSCLC. In addition, including additional NSCLC cell lines or primary tumor samples in future studies could enhance the generalizability of findings. These limitations will be further improved in our future research.

Conclusions

NAT10 regulated glycolysis and apoptosis in NSCLC via ac^4C acetylating ENO1, implying that NAT10 can be used as a biomarker to study the development and progression of NSCLC, or as a potential target for future treatment of NSCLC.

Abbreviations

ac ⁴ C	N4-Acetylcytidine
CCK-8	Cell counting kit-8
DMEM	Dulbecco's modified eagle's medium
ECAR	Extracellular acidification rate
ENO1	α -enolase
FBS	Fetal bovine serum
FDG	¹⁸ F-fluorodeoxyglucose
GAPDH	Glyceraldehyde-3-phosphate dehydrogenase
LUAD	Lung adenocarcinoma
LUSC	Lung squamous cell carcinoma
NAT10	N-Acetyltransferase 10
NSCLC	Non-small cell lung cancer
OCR	Oxygen consumption rate
RIP	RNA immunoprecipitation
RT-qPCR	Reverse transcription-quantitative polymerase chain reaction
shRNA	Short hairpin RNA
UALCAN	University of Alabama at Birmingham cancer data analysis portal

Acknowledgements

N/A.

Author contributions

DY conceived and designed the project, YY acquired the data, NL, JZ, CS and XZ analysed and interpreted the data, YY wrote the paper.

Funding

This study was supported by Regarding mir-145-5p targeting SOX2, it inhibits non-small cell lung cancer proliferation, metastasis, and angiogenesis through the Wnt/ β -Catenin signaling pathway. Project of Hunan Provincial Health Commission, No. 202203023122.

Data availability

The datasets used and/or analyzed during the current study are available from the corresponding author on reasonable request.

Declarations

Ethics approval and consent to participate

N/A.

Consent for publication

All authors approved the final manuscript and the submission to this journal.

Competing interests

The authors declare no competing interests.

Received: 10 October 2023 / Accepted: 27 December 2024

Published online: 13 February 2025

References

1. Ettinger DS, et al. NCCN Guidelines(R) Insights: Non-small Cell Lung Cancer, Version 2.2023. *J Natl Compr Canc Netw*. 2023;21(4):340–50.
2. Chen Z, et al. Non-small-cell lung cancers: a heterogeneous set of diseases. *Nat Rev Cancer*. 2014;14(8):535–46.
3. Wang M, Herbst RS, Boshoff C. Toward personalized treatment approaches for non-small-cell lung cancer. *Nat Med*. 2021;27(8):1345–56.
4. Gridelli C, et al. Gefitinib as first-line treatment for patients with advanced non-small-cell lung cancer with activating epidermal growth factor receptor mutation: review of the evidence. *Lung Cancer*. 2011;71(3):249–57.
5. Friedlaender A et al. Targeted therapies in Early Stage NSCLC: hype or hope? *Int J Mol Sci*. 2020. 21(17).
6. Wang X, et al. N6-methyladenosine-dependent regulation of messenger RNA stability. *Nature*. 2014;505(7481):117–20.
7. Meyer KD, et al. 5' UTR m(6)a promotes Cap-independent translation. *Cell*. 2015;163(4):999–1010.
8. Fustin JM, et al. RNA-methylation-dependent RNA processing controls the speed of the circadian clock. *Cell*. 2013;155(4):793–806.
9. Dong C, et al. tRNA modification profiles of the fast-proliferating cancer cells. *Biochem Biophys Res Commun*. 2016;476(4):340–5.
10. Castello A, et al. Insights into RNA biology from an atlas of mammalian mRNA-binding proteins. *Cell*. 2012;149(6):1393–406.
11. Tsai K, et al. Acetylation of cytidine residues boosts HIV-1 gene expression by increasing viral RNA Stability. *Cell Host Microbe*. 2020;28(2):306–e3126.
12. Nance KD, et al. Cytidine acetylation yields a hypoinflammatory synthetic messenger RNA. *Cell Chem Biol*. 2022;29(2):312–e3207.
13. Yang C, et al. Prognostic and immunological role of mRNA ac4C Regulator NAT10 in Pan-cancer: New Territory for Cancer Research? *Front Oncol*. 2021;11:630417.
14. Chen L, et al. NAT10-mediated N4-acetylcytidine modification is required for meiosis entry and progression in male germ cells. *Nucleic Acids Res*. 2022;50(19):10896–913.
15. Zheng N et al. Regulatory roles of NAT10 in airway epithelial cell function and metabolism in pathological conditions. *Cell Biol Toxicol*. 2022;39(4):1237–1256.
16. Wang Z, et al. c-myc-mediated upregulation of NAT10 facilitates tumor development via cell cycle regulation in non-small cell lung cancer. *Med Oncol*. 2022;39(10):140.
17. Wang Z, et al. NAT10-mediated upregulation of GAS5 facilitates immune cell infiltration in non-small cell lung cancer via the MYBBP1A-p53/IRF1/type I interferon signaling axis. *Cell Death Discov*. 2024;10(1):240.
18. Wang G, et al. NAT10-mediated mRNA N4-acetylcytidine modification promotes bladder cancer progression. *Clin Transl Med*. 2022;12(5):e738.
19. Deng M, et al. Helicobacter pylori-induced NAT10 stabilizes MDM2 mRNA via RNA acetylation to facilitate gastric cancer progression. *J Exp Clin Cancer Res*. 2023;42(1):9.
20. Liao L, et al. Lysine 2-hydroxyisobutyrylation of NAT10 promotes cancer metastasis in an ac4C-dependent manner. *Cell Res*. 2023;33(5):355–71.
21. Ganapathy-Kanniappan S, Geschwind JF. Tumor glycolysis as a target for cancer therapy: progress and prospects. *Mol Cancer*. 2013;12:152.
22. Akins NS, Nielson TC, Le HV. Inhibition of Glycolysis and glutaminolysis: an emerging drug Discovery Approach to Combat Cancer. *Curr Top Med Chem*. 2018;18(6):494–504.
23. Liu YC, et al. Pan-cancer analysis of clinical significance and associated molecular features of glycolysis. *Bioengineered*. 2021;12(1):4233–46.
24. Li W, et al. Comprehensive analysis of the association between tumor glycolysis and immune/inflammation function in breast cancer. *J Transl Med*. 2020;18(1):92.
25. Huang CK, et al. ENO1 and Cancer. *Mol Ther Oncolytics*. 2022;24:288–98.
26. Ma L, et al. The essential roles of m(6)a RNA modification to stimulate ENO1-dependent glycolysis and tumorigenesis in lung adenocarcinoma. *J Exp Clin Cancer Res*. 2022;41(1):36.
27. Li HJ, et al. ENO1 promotes Lung Cancer Metastasis via HGFR and WNT signaling-driven epithelial-to-mesenchymal transition. *Cancer Res*. 2021;81(15):4094–109.
28. Yan M, et al. RNA-binding protein KHSRP promotes tumor growth and metastasis in non-small cell lung cancer. *J Exp Clin Cancer Res*. 2019;38(1):478.
29. Lu J, et al. Ciclopirox targets cellular bioenergetics and activates ER stress to induce apoptosis in non-small cell lung cancer cells. *Cell Commun Signal*. 2022;20(1):37.
30. Zhang H, et al. The impaired Bioenergetics of Diabetic Cardiac Microvascular endothelial cells. *Front Endocrinol (Lausanne)*. 2021;12:642857.
31. Lin J, et al. NAT10 maintains OGA mRNA Stability through ac4C modification in regulating oocyte maturation. *Front Endocrinol (Lausanne)*. 2022;13:907286.
32. Pan Z, et al. Role of NAT10-mediated ac4C-modified HSP90AA1 RNA acetylation in ER stress-mediated metastasis and lenvatinib resistance in hepatocellular carcinoma. *Cell Death Discov*. 2023;9(1):56.
33. Zhang H, et al. NAT10 mediated mRNA acetylation modification patterns associated with colon cancer progression and microsatellite status. *Epi-genetics*. 2023;18(1):2188667.
34. Guo Q, et al. Remodelin delays non-small cell lung cancer progression by inhibiting NAT10 via the EMT pathway. *Cancer Med*. 2024;13(11):e7283.
35. Xu H, et al. N-alpha-acetyltransferase 10 protein inhibits apoptosis through RelA/p65-regulated MCL1 expression. *Carcinogenesis*. 2012;33(6):1193–202.
36. Yang Q et al. N4-Acetylcytidine drives glycolysis addiction in gastric Cancer via NAT10/SEPT9/HIF-1alpha positive feedback Loop. *Adv Sci (Weinh)*. 2023;10(23):e2300898.
37. Huang Z, et al. Identification of ENO1 as a prognostic biomarker and molecular target among ENOs in bladder cancer. *J Transl Med*. 2022;20(1):315.

38. Zhang H, et al. NAT10 regulates neutrophil pyroptosis in sepsis via acetylating ULK1 RNA and activating STING pathway. *Commun Biol.* 2022;5(1):916.

Publisher's note

Springer Nature remains neutral with regard to jurisdictional claims in published maps and institutional affiliations.